

## **Simulation and Measurement Considerations for Resonant Cavity Couplers and Extrapolating Results to Multiple Cells and Varying Conductivities**

T. Berenc, C. Deibele

**Abstract:** *The superconducting cavity for the kaon separator is being designed and built at FNAL. It is desired to design and optimize the coupling into a copper cavity and extrapolate these results to a superconducting multiple cell cavity. The theory for this procedure is outlined and the considerations for port placement and for simulation are presented.*

### **I. Introduction**

It is desired to design and build an input coupler for a multiple cell superconducting cavity resonator for the Kaon Separator at FNAL. The design of the coupler is tested using a copper model of the cavity, and the coupler is modeled using a finite element (FEM) electromagnetic code. It is required, therefore, to take the simulated and measured data and extrapolate the results to the superconducting case. The theory for this extrapolation procedure is presented. Additionally, practical concerns for the FEM code are shown. Finally, based on the theory presented in this paper, three different methods for finding the various cavity quality factors ( $Q$ 's) are shown.

### **II. Background and Theory**

#### **a. Definition of Planes**

In order to analyze the problem of coupling to a cavity, we assume a generic cavity and coupling as shown in Fig. 1. In this figure, a source excites a resonant cavity through some means of coupling; either electric, magnetic, or a combination of the two. The source, which is represented as a current source, is connected to the cavity through a transmission line with a characteristic impedance matched to the impedance of the source. Also represented in Fig. 1 are two planes of reference; the measurement/simulation plane and the detuned short plane. These reference planes are described

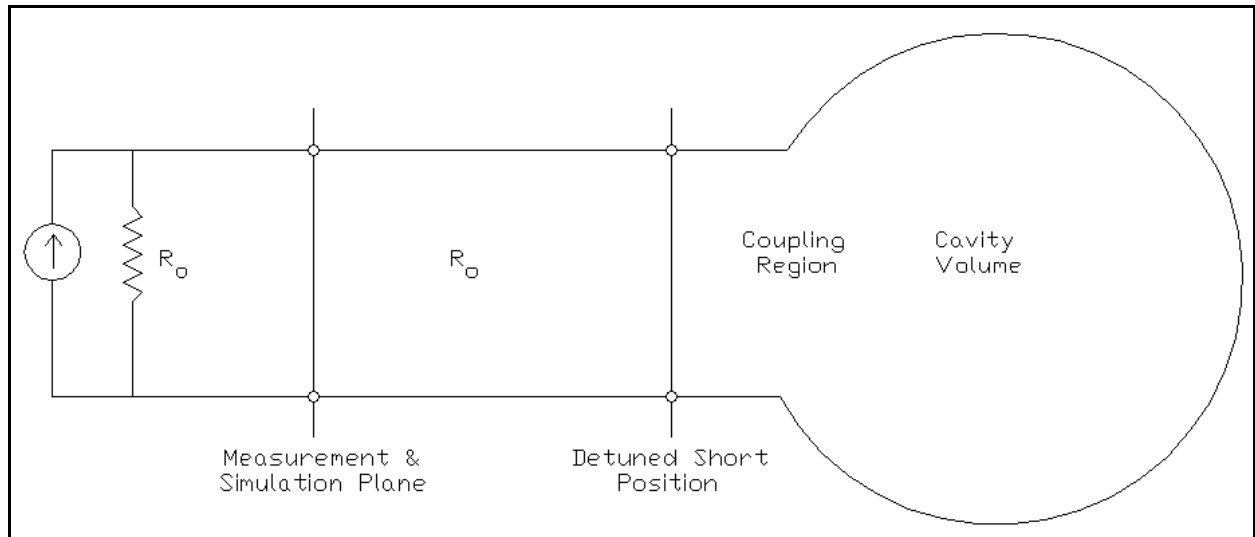


**Figure 1.** General schematic representing the coupling into a cavity resonator. The cavity is represented on the right. A general magnetic/electric field coupling is represented. The cavity is driven by a source on the right, which is matched to a transmission line which connects to the coupler.

below.

The measurement/simulation plane is the plane at which either physical measurements are taken or simulation results are obtained. In the case of both physical and simulated measurements, the measurement/simulation plane must be far enough away from the cavity such that the higher order modes (HOM's) at the coupler/cavity interface have sufficiently decayed. If the length of the coupling line is too short, HOM's can change the port impedance and will consequently affect estimates of the Q's. Additionally, the length of transmission line must be at least  $\lambda / 2$  away from the cavity boundary so that the FEM code has stabilized the solution of the fundamental transmission line mode.

The detuned short plane is the first position to the left of the cavity at which everything to the right of this detuned short plane can be modeled as a simple parallel RLC circuit. In other words, the impedance looking into the coupler and cavity at the detuned short plane behaves, as a function of frequency, like a parallel RLC circuit. It is the behavior of this RLC circuit which is of interest. The

parameters of this RLC circuit give a measurement of the coupling coefficient,  $\beta$ , and the Q of the volume to the right of the detuned short plane. It is important to note that the detuned short plane is a

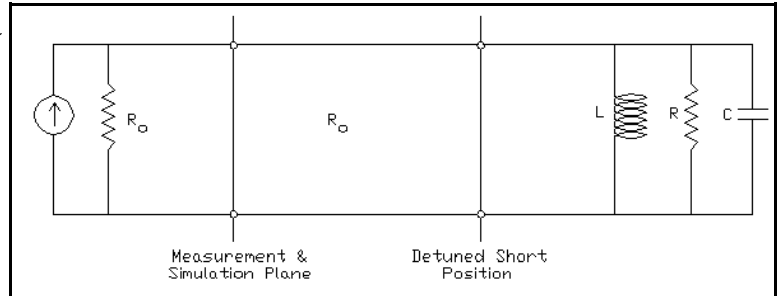


**Figure 2.** The circuit equivalent of the coupling problem described by Fig. 1.

fictitious plane of reference. This is to say that it incorporates the nonlinear reactance of the coupling structure with the impedance of the cavity resonator. If the coupling structure were to change in length by a set amount, the detuned short plane can change in either direction, either towards or away from, the cavity. The detuned short plane is described in detail by Ginzton<sup>1</sup>.

Replacing everything to the right of the detuned short plane by a parallel RLC circuit, our model now becomes that which is represented in Fig. 2. The values of L, C, and R are circuit quantities which describe the particular electromagnetic energy storage and losses for the cavity mode of interest.

Most situations involve measurement or simulation of the reflection coefficient,  $s_{11}$ , as a function of frequency at the measurement/simulation plane. The measurement/simulation data is notated as  $s_{11}^{meas}$ . In order to move to the plane of interest (the detuned short plane), the length of transmission line between the measurement/simulation plane and the detuned short plane is calibrated out. This is performed mathematically by

$$s_{11}^{cal}(f) = s_{11}^{meas}(f)e^{i2\pi ft_{delay}}. \quad (1)$$

---

<sup>1</sup>Microwave Measurements, E. L. Ginzton, McGraw-Hill Book Co., 1957, Library of Congress Catalog Number 56-13393, pp. 397-399.

The quantity  $t_{\text{delay}}$  is a constant and is chosen such that the resultant data, represents the reflection coefficient of a parallel RLC circuit. This is achieved by choosing  $t_{\text{delay}}$  such that:

- at the resonant frequency,
- $$s_{11}^{\text{cal}}(f_o) = \text{Re}(s_{11}^{\text{cal}}(f_o)e^{i2\pi f_o t_{\text{delay}}}) \text{ and}$$
- $s_{11}^{\text{cal}}(f)$  approaches a short circuit as the frequency immediately departs from the resonant frequency.

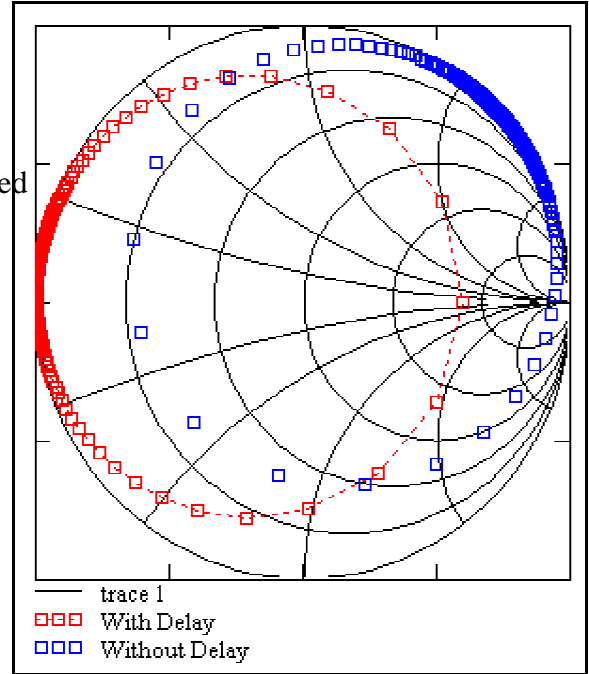


**Figure 3.** Typical simulated data for a cavity driven with a long transmission line. The delay

This second condition is usually ensured by visual inspection of the calibrated data in the Smith chart. In the Smith chart, the result of calibrating the  $s_{11}^{\text{meas}}$  data causes a rotation of the resonant circle<sup>2</sup> about the center of the Smith chart<sup>3</sup>. An example of this is portrayed in Fig. 3, where the blue trace is simulated reflection data and the red trace is the reflection calibrated data.

Once the reflection coefficient data has been calibrated, the circuit model of Fig. 4 becomes the reduced model of Fig. 3 in which both the length of transmission line between the measurement/simulation plane and the detuned short plane and the reactance of the coupling structure has been removed.

<sup>2</sup>A resonant RLC circuit is represented by a circle on the Smith chart. See G. Gonzales, “Microwave Transistor Amplifiers,” Prentice-Hall, Engelwood Cliffs, 1984, pp. 42-51.

<sup>3</sup>G. Gonzalez, “Microwave Transistor Amplifiers,” Prentice-Hall, Engelwood Cliffs, 1984, pp. 1-42.

### b. Circuit Model Descriptions and Quality Factor Definitions

The impedance of the parallel RLC can be normalized with respect to the source impedance and expressed in terms of its quality factor as

follows:

$$z(f) = \frac{Z_{RLC}(f)}{R_o} = \frac{\beta}{1 + i Q_o \left( \frac{f^2 - f_o^2}{f f_o} \right)}, \quad (2)$$

where  $Q_o$  is the unloaded quality factor of the parallel RLC circuit and is defined as:

$$Q_o = 2\pi \frac{\text{Energy Stored in Cavity}}{\text{Energy Lost in Cavity per cycle}} = 2\pi f_o RC,$$

and the other parameter

$$\beta = \frac{R}{R_o} \quad (3)$$

is defined as the coupling coefficient.

Two additional coupling and cavity parameters can be defined. The first is the loaded  $Q$ , or  $Q_L$ :

$$Q_L = 2\pi \frac{\text{Energy Stored in Cavity}}{\text{Total Energy Lost (Cavity plus Source) per cycle}} = 2\pi f_o R_{total} C,$$

where  $R_{total}$  is the parallel combination of  $R$  and  $R_o$ . The next parameter is the external  $Q$ , or  $Q_{ext}$ :

$$Q_{ext} = 2\pi \frac{\text{Energy Stored in Cavity}}{\text{Energy Lost to Source per cycle}} = 2\pi f_o R_o C.$$

$Q_{ext}$  is therefore a measure of the energy that leaves the cavity and is dissipated in the source impedance. Based upon the definitions of the various  $Q$ 's, the relationship between them is

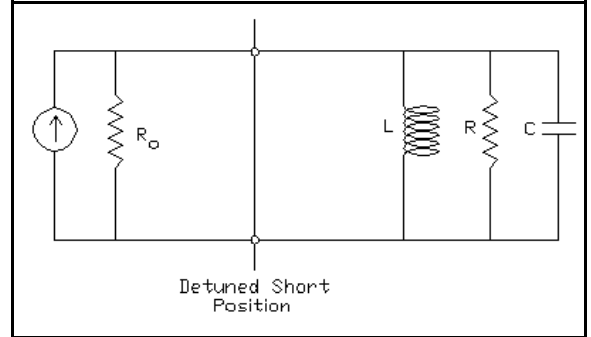


**Figure 4.** The resulting circuit from the rotation described by Eq. 1. This circuit has a real impedance presented to its source at the resonant frequency.

$$\frac{1}{Q_L} = \frac{1}{Q_o} + \frac{1}{Q_{ext}}. \quad (4)$$

Furthermore, further examination of Eq. 3 reveals that the coupling coefficient,  $\beta$ , is seen to be equal to the ratio of  $Q_o$  to  $Q_{ext}$ :

$$\beta = \frac{R}{R_o} = \frac{Q_o}{Q_{ext}}. \quad (5)$$

Inserting Eq. 5 into Eq. 4 reveals the relationship between  $Q_L$  and  $Q_o$ :

$$Q_o = Q_L(1 + \beta) \quad (6)$$

### c. Obtaining the Quality Factors from the Reflection Coefficient Data

For frequencies not too far from the resonant frequency, the term multiplying  $Q_o$  in the denominator of Eq. 2, can be approximated by the first two terms of a Taylor series expansion about  $f_o$ . Thus, the expression for the normalized impedance of the RLC circuit becomes,

$$z(f) \approx \frac{\beta}{1 + i2Q_o\delta(f)}, \quad (7a)$$

where  $\delta(f) = \left( \frac{f - f_o}{f_o} \right)$ . Equation 7 can be rewritten into a slightly different form using Eqs. 5-6:

$$z(f) \approx \frac{\beta}{1 + i2\beta Q_{ext}\delta(f)}, \quad (7b)$$

or as

$$z(f) \approx \frac{\beta}{1 + i2\beta Q_L(1 + \beta)\delta(f)}. \quad (7c)$$

Equations 7a-7c are convenient expressions to use for interpreting the  $s_{11}$  data. Each of the three expressions for  $z(f)$  leads to a different method by which to calculate all of the Q factors from the  $s_{11}$  data. Each of these methods assumes that the resonant frequency is found from the point at which the magnitude of  $s_{11}^{cal}$  is minimum. Each method also assumes that  $\beta$  is calculated from the value of  $s_{11}^{cal}(f_o)$  in the following way:

$$\beta = \frac{1 + s_{11}^{cal}(f_o)}{1 - s_{11}^{cal}(f_o)}. \quad (8)$$

Recall that the calibrated reflection coefficient at the resonant frequency is purely real, and hence so is the coupling coefficient.

Since the reflection coefficient is measured/simulated at discrete frequency points, a piecewise continuous function is created for use with the three different methods. This piecewise continuous function, notated as  $\Gamma(f)$ , is defined as:

$$\Gamma(f) = \sum_{s=0}^{numpts-1} \Theta(f, s) \left( \frac{s_{11}(f_{s+1}) - s_{11}(f_s)}{f_{s+1} - f_s} (f - f_s) + s_{11}(f_s) \right),$$

where

$$\Theta(f, s) = \begin{cases} 0 & f < f_s \\ 1 & f_s \leq f \leq f_{s+1} \\ 0 & f_{s+1} < f \end{cases}$$

$numpts$  are the number of frequency points that the FEM solver calculates, and the  $f_s$  are the frequency points that the FEM solver generates or the frequency points where the measurements are made using a vector network analyzer. This function allows a more precise calculation of the critical parameters which describe the coupling and losses associated with the coupling and in the bulk material itself.

### **i. Calculation by First Finding $Q_0$**

The first method by which to calculate the various Q factors is to use Eq. 7a. At a certain frequency,  $f_{+Q_0}$ , the denominator becomes equal to  $(1 + i)$ . Similarly, there is another frequency,  $f_{-Q_0}$ , at which the denominator becomes equal to  $(1 - i)$ . At these frequencies, the normalized impedance can be written as

$$z(f_{\pm Q_0}) = \frac{\beta}{1 \pm i}.$$

Thus, the following two equations are satisfied by frequencies  $f_{+Q_0}$  and  $f_{-Q_0}$ :

$$\text{Im}\left(z(f_{-Q_0})\right) = \text{Re}\left(z(f_{-Q_0})\right) \quad \text{or} \quad -\text{Im}\left(z(f_{+Q_0})\right) = \text{Re}\left(z(f_{+Q_0})\right).$$

Determining the frequency,  $f_{-Q_0}$ , is equivalent to finding the intersection of the interpolated function,  $\Gamma(f)$ , with the locus of all points for which  $\text{Im}(z)=\text{Re}(z)$ . Similarly, finding the frequency,  $f_{+Q_0}$ , is equivalent to finding the intersection of  $\Gamma(f)$  with the locus of all points for which  $-\text{Im}(z)=\text{Re}(z)$ . This is mathematically equivalent to finding the roots of the equation

$$\text{Im}\left(\frac{1+\Gamma(f)}{1-\Gamma(f)}\right) \pm \text{Re}\left(\frac{1+\Gamma(f)}{1-\Gamma(f)}\right) = 0.$$

A pictorial representation of this intersection in the Smith chart is shown in Figure 5. Either  $f_{-Q_0}$  or  $f_{+Q_0}$  can then be used to calculate  $Q_0$ :

$$Q_0 = \frac{f_o}{2|f_o - f_{\pm Q_0}|}.$$

Once  $Q_0$  is calculated,  $Q_{ext}$  follows from Eq. 5:

$$Q_{ext} = \frac{Q_0}{\beta}.$$

Finally,  $Q_L$  can then be calculated using Eq. 4 as

$$Q_L = \frac{Q_0 Q_{ext}}{Q_0 + Q_{ext}}.$$

## ii. Calculation by First Finding $Q_{ext}$

The second method by which to calculate the various Q factors is to use Eq. 7b. Following similar logic as outlined as in part ii, at a certain frequency,

$f_{+Q_{ext}}$  the denominator becomes equal to  $(1 + i\beta)$ .

Similarly, there is another frequency,  $f_{-Q_{ext}}$ , at which

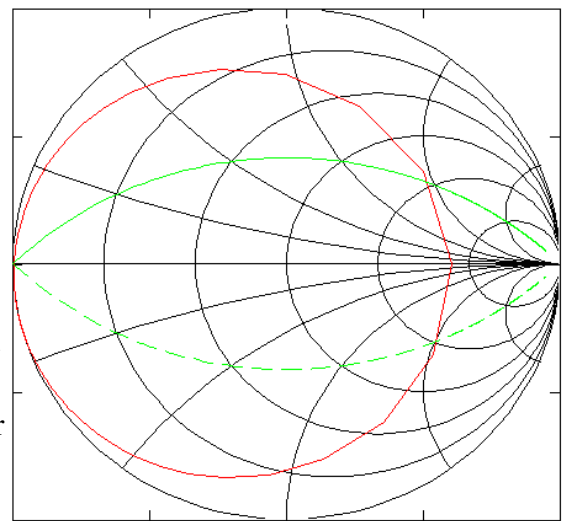


**Figure 5.** Smith chart for finding the  $Q_0$  for a calculated data set (red curve). The frequencies where the  $\text{Re}(z(f))=\pm\text{Im}(z(f))$  (green curves) intersect define the unloaded Q.

the denominator becomes equal to  $(1 - i\beta)$ . At these frequencies, the normalized impedance can be written as

$$z(f_{\pm Q_{ext}}) = \frac{\beta}{1 \pm i\beta},$$

or equivalently, the normalized admittance, given as  $y(f) = \frac{1}{z(f)}$ , can be written as

$$y(f_{\pm Q_{ext}}) = \frac{1}{\beta} \pm i.$$

Thus, the following two equations are satisfied by frequencies  $f_{+Q_{ext}}$  and  $f_{-Q_{ext}}$ :

$$\text{Im}\left(y(f_{-Q_{ext}})\right) = -1 \quad \text{or} \quad \text{Im}\left(y(f_{+Q_{ext}})\right) = 1.$$

Finding the frequency,  $f_{-Q_{ext}}$ , is equivalent to finding the intersection of the interpolated function,  $\Gamma(f)$ , with the locus of all points for which  $-\text{Im}(y)=1$ . Similarly, finding the frequency,  $f_{+Q_{ext}}$ , is equivalent to finding the intersection of  $\Gamma(f)$  with the locus of all points for which  $\text{Im}(y)=1$ . This is mathematically equivalent to finding the roots of the equation

$$\text{Im}\left(\frac{1 - \Gamma(f)}{1 + \Gamma(f)}\right) \pm 1 = 0.$$

A pictorial representation of this intersection in the

Smith Chart is shown in Fig. 6. Either  $f_{-Q_{ext}}$  or

$f_{+Q_{ext}}$  can then be used to calculate  $Q_{ext}$ :

$$Q_{ext} = \frac{f_o}{2|f_o - f_{\pm Q_{ext}}|}.$$

Once  $Q_{ext}$  is calculated,  $Q_o$  follows from Eq. 5:

$$Q_o = \beta Q_{ext}.$$

Finally,  $Q_L$  can then be calculated using Eq. 4 as

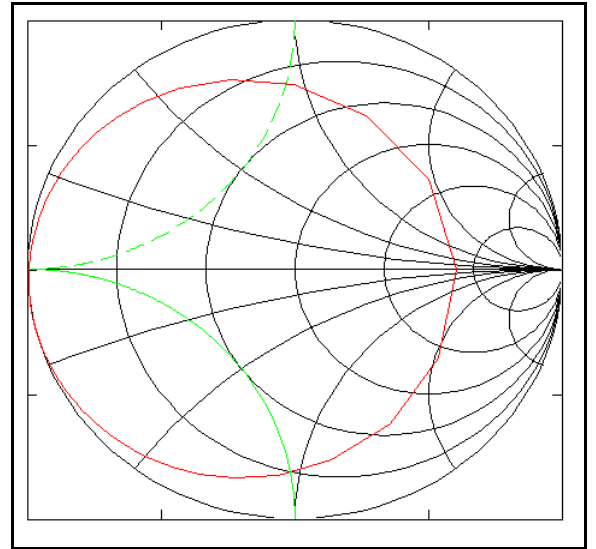


**Figure 6.** The calculated reflection data (red curve) intersect with the lines of  $\text{Im}(y)=\pm 1$ . The frequencies where this intersection occurs defines the  $Q_{ext}$ .

$$Q_L = \frac{Q_o Q_{ext}}{Q_o + Q_{ext}}.$$

### iii. Calculation by First Finding $Q_L$

The third method by which to calculate the various Q factors is to use Eq. 7c. Again, following a similar logic as in parts i and ii, at a certain frequency,  $f_{+QL}$ , the denominator becomes equal to  $(1 + i(1 + \beta))$ . Similarly, there is another frequency,  $f_{-QL}$ , at which the denominator becomes equal to  $(1 - i(1 + \beta))$ . At these frequencies, the normalized impedance can be written as

$$z(f_{\pm QL}) = \frac{\beta}{1 \pm i(1 + \beta)},$$

or equivalently, the normalized admittance, given as  $y(f) = \frac{1}{z(f)}$ , can be written as

$$y(f_{\pm QL}) = \frac{1}{\beta} \pm i \left( \frac{1}{\beta} + 1 \right).$$

Thus, the following two equations are satisfied by frequencies  $f_{+QL}$  and  $f_{-QL}$ :

$$\text{Im}\left(y(f_{-QL})\right) = -\text{Re}\left(y(f_{-QL}) + 1\right) \quad \text{or} \quad \text{Im}\left(y(f_{+QL})\right) = \text{Re}\left(y(f_{+QL}) + 1\right).$$

Finding the frequency,  $f_{-Q_{ext}}$ , is equivalent to finding the intersection of the interpolated function,  $\Gamma(f)$ , with the locus of all points for which  $-\text{Im}(y) = \text{Re}(y+1)$ . Similarly, finding the frequency,  $f_{+Q_{ext}}$ , is equivalent to finding the intersection of  $\Gamma(f)$  with the locus of all points for which  $\text{Im}(y) = \text{Re}(y+1)$ . This is mathematically equivalent to finding the roots of the equation

$$\text{Im}\left(\frac{1 - \Gamma(f)}{1 + \Gamma(f)}\right) \pm \text{Re}\left(\frac{1 - \Gamma(f)}{1 + \Gamma(f)} + 1\right) = 0.$$

A pictorial representation of this intersection in the Smith chart is shown in Figure 7. Either  $f_{-QL}$  or  $f_{+QL}$  can then be used to calculate  $Q_L$ :

$$Q_L = \frac{f_o}{2|f_o - f_{\pm Q_L}|}$$

Once  $Q_L$  is calculated,  $Q_o$  follows from Eq. 6:

$$Q_o = Q_L(1 + \beta).$$

Finally,  $Q_{ext}$  can then be calculated using Eq. 5 as

$$Q_{ext} = \frac{Q_o}{\beta}.$$

#### d. Extrapolating the Normal Conductivity Results to Superconducting and to Multi-cell

The results shown in this paper discuss only a single cell. It is desired, however, to extrapolate the single cell results to a multi-cell cavity resonator which is super conducting. This extrapolation is straightforward using the theory which describes each individual Q.

The first assumption one must make with the superconducting resonator is that the unloaded Q of the superconducting cavity is on the order of  $10^9$  or  $10^{10}$ . These numbers are arrived at from previous measurements made with similar cavities. Since the Kaon Separator requires a particular  $Q_L$ , it will be shown later that the unloaded Q of the superconducting cavity is minimally involved in the loaded Q.

The external Q is unaffected by the conductivity of the material. Recall that the external Q is a measure of energy storage to energy propagating through the input port. The energy storage remains

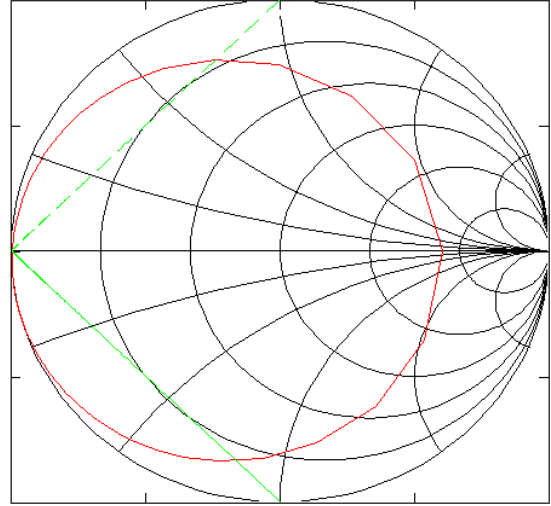


**Figure 7.** Smith chart showing the intersection of a resonance curve (red) with lines satisfying  $\text{Im}(y) = \pm(\text{Re}(y) + 1)$ . The frequencies that satisfy this relationship define the  $Q_L$ .

constant<sup>4</sup>, and since the geometry remains constant (only the conductivity changes), the energy coupled to the input port also remains constant. Therefore, the external Q must remain constant.

If one allows multiple cavities to be present, we assume that we operate the cavity in such a manner that each cell of the cavity has identical fields. In this manner, the stored energy of the n-cell cavity is n times greater than the single cell case while the energy coupled to the single input port remains fixed. Therefore, the external Q of the n-cell cavity is n times greater than a single cell

$$Q_{ext-n} = nQ_{ext} \quad (9)$$

From these three assumptions, the loaded Q of an n-cell superconducting cavity can be estimated using Eq. 3:

$$Q_{L-niobium} = \frac{nQ_{ext}Q_{o-niobium}}{nQ_{ext} + Q_{o-niobium}} \Rightarrow Q_{L-niobium} = 10^9 \times nQ_{ext} (10^9 + nQ_{ext})^{-1} \approx nQ_{ext} \left( 1 - \frac{nQ_{ext}}{10^9} \right)^{-1}.$$

This shows that the  $Q_L$  of the niobium is inversely proportional to the  $Q_o$  of a multi-cell cavity, while the number of cells and the  $Q_{ext}$  are the dominant factors in determining the  $Q_L$  of a superconducting cavity.

## v. Summary of Theory for Calculating Q's

The methods for calculating the appropriate Q's have been summarized so it is possible to compare the results from each method and to ensure that an appropriate number of frequency points have been calculated near the actual resonant frequency of the structure. As the conductivity of resonant structure increases, it becomes increasingly important to find the correct resonant frequency

---

<sup>4</sup>This is a common assumption in perturbation theory. It is typical that one solves for the perfectly conducting cavity first, then based on the tangential magnetic field, it is possible to determine the losses in the highly conductive problem. See, for example, R. Harrington, "Time-Harmonic Electromagnetic Fields," Mc-Graw Hill Book Co., 1961, Library of Congress Catalog # 60-14221, pp. 208-216 and pp. 372-373.

since the resonant frequency is implicitly used at each step of the estimation procedure. This effect can be minimized by choosing a dense mesh of frequency points about the resonant frequency of the cavity.

### **III. Summary**

It is not always desirable to simulate a problem or build a structure using the desired conductivity of the material. The methods presented in this paper show how one can extrapolate from one conductivity to another relatively easily and straightforwardly. It is required, however, that a good set of data exists and that the conductivity is high enough such that the estimates used in this paper are reasonable. Additionally, if the mode of interest for a multiple cell cavity has uniform energy density from cell to cell, it is also possible to extrapolate how the Q's should behave in this scenario.